2021

Regulation of beta-amyloid production in neurons by astrocyte-derived cholesterol

Hao Wang

Joshua A. Kulas

Chao Wang

David M. Holtzman

Heather A. Ferris

See next page for additional authors

Authors

Hao Wang, Joshua A. Kulas, Chao Wang, David M. Holtzman, Heather A. Ferris, and Scott B. Hansen

Regulation of beta-amyloid production in neurons by astrocyte-derived cholesterol

Hao Wang[a,b,c,1], Joshua A. Kulas[d,e,1], Chao Wang[f], David M. Holtzman[f], Heather A. Ferris[d,e,2], and Scott B. Hansen[a,b,2]

[a]Department of Molecular Medicine, The Scripps Research Institute, Jupiter, FL 33458; [b]Department of Neuroscience, The Scripps Research Institute, Jupiter, FL 33458; [c]Skaggs Graduate School of Chemical and Biological Sciences, The Scripps Research Institute, Jupiter, FL 33458; [d]Division of Endocrinology and Metabolism, University of Virginia, Charlottesville, VA 22908; [e]Department of Neuroscience, University of Virginia, Charlottesville, VA 22908; and [f]Department of Neurology, Hope Center for Neurological Disorders, Knight Alzheimer's Disease Research Center, Washington University School of Medicine, St. Louis, MO 63110

Edited by Lawrence S. Goldstein, Sanford Consortium for Regenerative Medicine, La Jolla, CA, and approved June 23, 2021 (received for review February 3, 2021)

Alzheimer's disease (AD) is characterized by the presence of amyloid β (Aβ) plaques, tau tangles, inflammation, and loss of cognitive function. Genetic variation in a cholesterol transport protein, apolipoprotein E (apoE), is the most common genetic risk factor for sporadic AD. In vitro evidence suggests that apoE links to Aβ production through nanoscale lipid compartments (lipid clusters), but its regulation in vivo is unclear. Here, we use superresolution imaging in the mouse brain to show that apoE utilizes astrocyte-derived cholesterol to specifically traffic neuronal amyloid precursor protein (APP) in and out of lipid clusters, where it interacts with β- and γ-secretases to generate Aβ-peptide. We find that the targeted deletion of astrocyte cholesterol synthesis robustly reduces amyloid and tau burden in a mouse model of AD. Treatment with cholesterol-free apoE or knockdown of cholesterol synthesis in astrocytes decreases cholesterol levels in cultured neurons and causes APP to traffic out of lipid clusters, where it interacts with α-secretase and gives rise to soluble APP-α (sAPP-α), a neuronal protective product of APP. Changes in cellular cholesterol have no effect on α-, β-, and γ-secretase trafficking, suggesting that the ratio of Aβ to sAPP-α is regulated by the trafficking of the substrate, not the enzymes. We conclude that cholesterol is kept low in neurons, which inhibits Aβ accumulation and enables the astrocyte regulation of Aβ accumulation by cholesterol signaling.

Alzheimer's | neurodegeneration | apoE | cholesterol | lipids

Alzheimer's disease (AD), the most prevalent neurodegenerative disorder, is characterized by the progressive loss of cognitive function and the accumulation of amyloid β (Aβ) peptide and phosphorylated tau (1). Amyloid plaques are composed of aggregates of Aβ peptide, a small hydrophobic protein excised from the transmembrane domain of amyloid precursor protein (APP) by proteases known as beta- (β-) and gamma- (γ-) secretases (*SI Appendix*, Fig. S1*A*). In high concentrations, Aβ peptide can aggregate to form Aβ plaques (2–4). The nonamyloidogenic pathway involves a third enzyme, alpha- (α-) secretase, which generates a soluble APP fragment (sAPP-α), helps set neuronal excitability in healthy individuals (5), and does not contribute to the generation of amyloid plaques. Therefore, by preventing Aβ production, α-secretase–mediated APP cleavage reduces plaque formation. Strikingly, both pathways are finely regulated by cholesterol (6) (*SI Appendix*, Fig. S1*B*).

In cellular membranes, cholesterol regulates the formation of lipid clusters (also known as lipid rafts) and the affinity of proteins to lipid clusters (7), including β-secretase and γ-secretase (8–10). α-secretase does not reside in lipid clusters; rather, α-secretase is thought to reside in a region made up of disordered polyunsaturated lipids (11). The location of APP is less clear. In detergent-resistant membrane (DRM) studies, it primarily associates with lipid from the disordered region, although not exclusively (8, 10, 12–14). Endocytosis is thought to bring APP in proximity to β-secretase and γ-secretase, and this correlates with Aβ production. Cross-linking of APP with β-secretase on the plasma membrane also increases Aβ production, leading to a hypothesis that lipid clustering in the membrane contributes to APP processing (11, 14, 15) (*SI Appendix*, Fig. S1*A*). Testing this hypothesis in vivo has been hampered by the small size and transient nature of lipid clusters (often <100 nm), which is below the resolution of light microscopy.

Superresolution imaging has emerged as a complimentary technique to DRMs, with the potential to interrogate cluster affinity more directly in a native cellular environment (16). We recently employed superresolution imaging to establish a membrane-mediated mechanism of general anesthesia (17). In that mechanism, cholesterol causes lipid clusters to sequester an enzyme away from its substrate. Removal of cholesterol then releases and activates the enzyme by giving it access to its substrate (*SI Appendix*, Fig. S1*C*) (7, 18). A similar mechanism has been proposed to regulate the exposure of APP to its cutting enzymes (11, 15, 19–21).

Neurons are believed to be the major source of Aβ in normal and AD brains (22, 23). In the adult brain, the ability of neurons to produce cholesterol is impaired (24). Instead, astrocytes make cholesterol and transport it to neurons with apolipoprotein E

Significance

The accumulation of amyloid β (Aβ) in the brain appears to be a necessary event in the pathogenesis of Alzheimer's disease (AD). However, processes linked to the endogenous regulation of Aβ production are still not completely understood. Here, the authors show that Aβ accumulation in neurons is tightly regulated by cholesterol synthesis and apoE transport from astrocytes. The study provides a molecular context for understanding the endogenous regulation of Aβ accumulation and why it correlates with AD. The tight regulation suggests that Aβ may perform an important cellular function. A complete understanding of the mechanism is likely necessary to predict whether the selective removal of Aβ has potential for a therapeutic benefit.

Author contributions: H.W., J.A.K., H.A.F., and S.B.H. designed research; H.W., J.A.K., and C.W. performed research; H.W., J.A.K., C.W., D.M.H., H.A.F., and S.B.H. analyzed data; D.M.H., H.A.F., and S.B.H. contributed the resources; and H.W., J.A.K., C.W., D.M.H., H.A.F., and S.B.H. wrote the paper.

Competing interest statement: D.M.H. is an inventor on a patent licensed by Washington University to C2N Diagnostics on the therapeutic use of anti-tau antibodies. D.M.H. cofounded and is on the scientific advisory board of C2N Diagnostics. C2N Diagnostics has licensed certain anti-tau antibodies to AbbVie for therapeutic development. D.M.H. is on the scientific advisory board of Denali and consults for Genentech, Merck, Cajal Neuroscience, and Eli Lilly.

This article is a PNAS Direct Submission.

[1]H.W. and J.A.K. contributed equally to this work.

[2]To whom correspondence may be addressed. Email: hf4f@virginia.edu or shansen@scripps.edu.

This article contains supporting information online at https://www.pnas.org/lookup/suppl/doi:10.1073/pnas.2102191118/-/DCSupplemental.

Published August 12, 2021.

(apoE) (25–27). Interestingly, apoE, specifically the e4 subtype (apoE4), is the strongest genetic risk factor associated with sporadic AD (28, 29). This led to the theory that astrocytes may be controlling Aβ accumulation through regulation of the lipid cluster function (11, 15, 19), but this has not yet been shown in the brain of an animal. Here, we show that astrocyte-derived cholesterol controls Aβ accumulation in vivo and links apoE, Aβ, and plaque formation to a single molecular pathway.

Results

Characterization of Astrocyte-Derived Cholesterol on Neuronal Cluster Formation. To establish a role for Aβ regulation by astrocytes in vivo, we first labeled and imaged monosialotetrahexosylganglioside1 (GM1) lipids in wild-type (WT) mouse brain slices. GM1 lipids reside in cholesterol-dependent lipid clusters and bind cholera toxin B (CTxB) with high affinity (30, 31). These GM1 domains are separate from phosphatidylinositol 4,5 bisphosphate domains, which are polyunsaturated and cholesterol independent (18, 32, 33). We labeled GM1 domains (i.e., lipid clusters) from cortical slices with Alexa Fluor 647–conjugated, fluorescent CTxB and imaged with confocal and superresolution direct stochastical optical reconstruction microscopy (dSTORM) (34–37). dSTORM is capable of visualizing nanoscale arrangements [i.e., sub–100-nm diameter lipid domain structures (38)] in intact cellular membranes.

CTxB appeared to label most cell types in cortical brain slices (*SI Appendix*, Fig. S2*A*, green shading). In neurons, labeled with a neuron-specific antibody against neurofilament medium (NFM) chain protein, CTxB can be seen outlining the plasma membrane (outside of the cell), as opposed to NFM which labels throughout the cells (*SI Appendix*, Fig. S2 *A*, *Right*).

Next, we investigated the role of cholesterol on the relative size and number of neuronal GM1 domains in brain tissue (Fig. 1*A*) using dSTORM (a ∼10-fold increase in resolution compared to confocal). In WT mouse cortical tissue, GM1 domains averaged ∼141 nm in apparent diameter, slightly smaller than the apparent size in primary neurons (∼150-nm diameter) (Fig. 1*B*). Cultured neuroblastoma 2a (N2a) cells exhibited the smallest clusters by far, on average only 100 nm in apparent diameter. All of the mammalian cells had domains larger than an intact fly brain, which had an apparent diameter of ∼90 nm (17). CTxB is pentadentate and can affect the absolute size; here, we used the numbers merely as a relative comparison of size under identical conditions (*SI Appendix*).

In order to determine if astrocytes were a key cholesterol source regulating GM1 lipid domains, we compared the size of GM1 domains in neurons cocultured with cholesterol-deficient astrocytes. We depleted astrocyte cholesterol by SREBP2 gene ablation ($SREBP2^{-/-}$). SREBP2 is an essential regulator of cholesterol synthesis enzymes (39) and was specifically knocked out in astrocytes using an ALDH1L1 promoter-driven Cre recombinase (40). We found that when cholesterol was depleted from astrocytes, the cluster size of primary neurons was significantly reduced (130 nm). The observed effect of astrocyte SREBP2 ablation on neurons suggests the decreased cholesterol transport to neurons—presumably through apoE.

To confirm that astrocytes could regulate neuronal GM1 domain formation through apoE, we added purified apoE to cultured primary neurons and N2a cells. The apoE (human subtype 3) derived from *Escherichia coli* was devoid of cholesterol, as prokaryotes do not make cholesterol. To provide a source of cholesterol to the apoE, we added 10% fetal bovine serum (FBS), a common source of mammalian lipids, including ∼310 μg/mL cholesterol-containing lipoproteins. ApoE can both load and unload cholesterol from cells, including neurons (41–43) (see also *SI Appendix*). To confirm apoE's effect in transporting cholesterol, we incubated apoE with N2a cells and analyzed the extracted lipids with mass spectrometry. The main apoE component extracted from the cells is cholesterol, including free cholesterol and cholesterol ester (Fig. 1*C*). Importantly, apoE is not present in FBS (44). Cells were treated acutely (1 h) with 4 μg/mL apoE, a physiologically relevant concentration seen in cerebral spinal fluid (45).

Loading cells with cholesterol (apoE and +FBS) caused an increase in the apparent cluster diameter from 100 to 130 nm in N2a cells (Fig. 1*D*). When cholesterol was unloaded, (ApoE absent a cholesterol source), the apparent size and number of GM1 domains decreased (Fig. 1 *D* and *E* and *SI Appendix*, Fig. S2*B*). Binning clusters by large >500 nm and small <150 nm showed a clear shift toward smaller domains, with apoE in low cholesterol, and a clear shift to large domains, with apoE in high cholesterol (*SI Appendix*, Fig. S2 *C* and *D*). We also measured cholesterol extraction by apoE in N2a cells using a quantitative absorbance assay. ApoE decreased the total cholesterol by ∼5% (*SI Appendix*, Fig. S2*E*). To confirm this result, we compared apoE treatment to treatment with methyl β-cyclodextrin (MβCD), a nonnative chemical binder that extracts cholesterol from the plasma membrane and disrupts cluster function (46). MβCD caused a similar decrease, as seen for cells with cholesterol effluxed (*SI Appendix*, Fig. S2 *O* and *P*).

We also investigated apoE's effect in modulating membrane cholesterol level and lipid cluster integrity using an enzymatic cluster disruption assay. The disruption assay uses phospholipase D (PLD) as a reporter of cluster disruption (18). After 1 h incubation with apoE (−Chol), PLD activity significantly increased, confirming cluster disruption (*SI Appendix*, Fig. S2*F*). We confirmed that apoE decreased the N2a total cellular cholesterol in the plasma membrane (Fig. 1*F*) using a live cell fluorescent cholesterol assay (see *Materials and Methods*). When incubated with cholesterol, apoE loads cholesterol into the cells. These results suggest a functional role of apoE in extracting/loading cellular cholesterol and modulate lipid clusters in cellular membranes. The live cell assay reduces pipetting errors and allows for a precise comparison of a treatment versus its control (Fig. 1*F*).

Superresolution Imaging of Amyloid-Processing Proteins in Lipid Clusters. Next, we sought to characterize a cellular function of cholesterol loading (i.e., the ability of GM1 domains to move APP toward or away from its hydrolyzing secretases). To establish the movement of APP to each of its processing enzymes, α-, β-, and γ-secretases, directly in cellular membranes, we imaged N2a cells with dSTORM. APP was previously found in both cluster- and noncluster-like fractions of DRMs (8, 10, 12–14). DRMs are similar to GM1 lipid clusters. However, imaging APP is important, since the amount of cluster-like association in DRMs could easily be affected by the detergent concentration used for preparation. We labeled GM1 domains with fluorescent CTxB and the amyloid proteins (APP, α-, β-, and γ -secretases) with Cy3b-labeled, fluorescent antibodies and determined cluster localization by pair correlation using density-based spatial clustering of applications with noise of two-color dSTORM images (Fig. 2*A*).

Fig. 2*B* shows that APP, β-secretase, and γ-secretase are associated with GM1 clusters (i.e., they exhibit strong pair correlation with CTxB-labeled GM1 lipids at short distances [5 nm]), consistent with experiments in DRMs.

In contrast, α-secretase is not associated with GM1 domains (i.e., lacks pair correlation with CTxB) (Fig. 2*B*). The pair correlation (a unitless number) ranged from 10 to 15 for APP, β-secretase, and γ-secretase, while the pair correlation for α-secretase was <3, a value typical for little or no pair correlation, a result also consistent with previous experiments in DRMs (15).

Cellular Regulation of APP Exposure to α- and β-Secretase by apoE. We then investigated the ability of apoE to mediate the delivery of cholesterol to cell membranes and regulate Aβ production in N2a cells. We applied 4 μg/mL human apoE isoform 3 (apoE3), purified from *E. coli* with and without cholesterol, and measured APP localization to lipid clusters with dSTORM. We found that

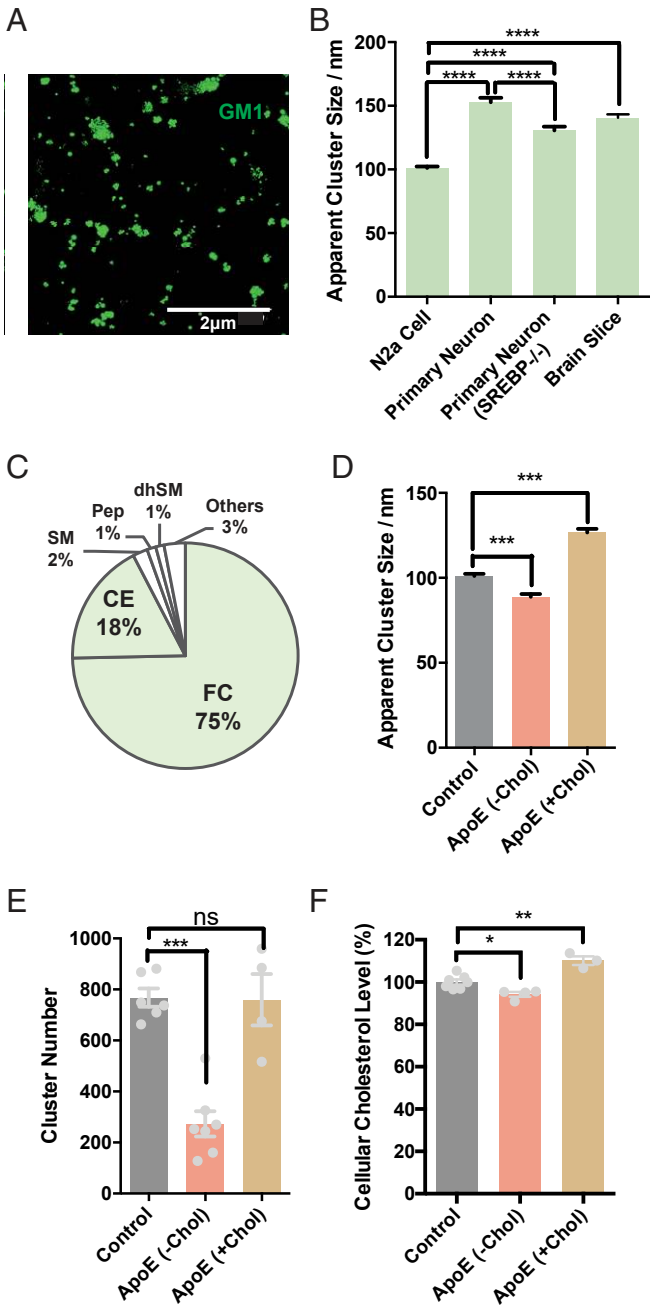

Fig. 1. Astrocyte cholesterol signals to membrane nanostructure in neurons. (*A*) dSTORM superresolution imaging on WT brain slices showing lipid cluster nanostructure in cell membrane. (Scale Bar, 2 μm.) (*B*) Comparison of apparent cluster length in N2a cells; primary neurons cultured with astrocytes with and without ($SREBP^{-/-}$) cholesterol synthesis and brain slices. Data are expressed as mean ± SEM and n = 1,748 to 6,779 clusters from >3 images. (*C*) Mass spectrometry analysis showing that the majority of lipids extracted by apoE (a cholesterol transport protein) from N2a cells are cholesterol. Some cluster-associated lipids are also transported by apoE. Abbreviations for lipids: FC, free cholesterol; CE, cholesterol ester; SM, sphingomyelin; dhSM, dihydrosphingomyelin; and Pep, plasmalogen phosphatidylethanolamine. (*D*) Quantitation of cluster lengths in N2a cells indicates changes in cluster structure after apoE treatment with and without a source of cholesterol (± chol). Data are expressed as mean ± SEM and n = 1,911 to 6,779 clusters from four to seven cells. (*E*) Quantitation of GM1 clusters in N2a cells shows that apoE decreased the number of clusters under low-cholesterol conditions, while apoE treatment with high, environmental cholesterol doesn't affect cluster number. Data are expressed as mean ± SEM and one-way ANOVA. (*F*) Exposure of N2a cells to apoE removes cholesterol from cellular membranes, as measured by a fluorescent-based live cell cholesterol assay. Cholesterol loading by apoE increases cellular cholesterol level. Data are expressed as mean ± SEM, n = 4 to 7, one-way ANOVA, $^{*}P < 0.05$, $^{***}P < 0.001$, and $^{****}P < 0.0001$.

when ApoE loaded cholesterol into cells (apoE +FBS), APP association with GM1 domains was almost twofold higher than when apoE effluxed cholesterol (apoE and −FBS) (Fig. 2 *C–E* and *SI Appendix*, Fig. S2 *G* and *H*). In a control experiment, FBS alone (+Chol with no apoE added) did not increase APP trafficking to lipid clusters (Fig. 2 *C* and *D* and *SI Appendix*, Fig. S2 *G* and *H*), confirming that apoE is a specific and necessary mediator of cholesterol transport to the neuron. This result also confirms previous mass spectrometry results (44) that there is no appreciable apoE in FBS—if apoE were already present, then adding more would not have had such a dramatic effect. Moreover, apoE alone (under low-cholesterol condition [−FBS]) decreased APP clustering (Fig. 2 *B* and *C* and *SI Appendix*, Fig. S2*G*), confirming that exogenously added apoE can unload cholesterol in neuronal membranes. ApoE efflux was similar to MβCD treatment (*SI Appendix*, Fig. S2 *O–S*) (11, 15).

Surprisingly, neither cholesterol loading nor the unloading of N2a cells had a significant effect on α-, β-, or γ-secretase trafficking in or out of GM1 domains (Fig. 2*E* and *SI Appendix*, Fig. S2 *I–N*). GM1 domains were analyzed pairwise for association with either α-, β-, or γ-secretase in an identical manner to APP. In contrast to APP, cholesterol unloading with apoE treatment was insufficient to move β- or γ-secretase out of GM1 domains. Likewise, more cholesterol failed to increase the association of any of the secretases. α-secretase, located in the disordered region, remained in the disordered region (Fig. 2 *B* and *E* and *SI Appendix*, Fig. S2 *I* and *J*), while β- and γ-secretases, which were already in the lipid clusters, did not increase their association with GM1 lipids in cholesterol-loaded cells (Fig. 2 *B* and *E* and *SI Appendix*, Fig. S2 *K–N*). This suggests that a mobile substrate (APP) moves between relatively static enzymes (secretases) in the plasma membrane. An enzyme-linked immunosorbent assay (ELISA) confirmed a shift from Aβ40 to sAPP-α production under low-cholesterol condition and increased Aβ40 generation in high-membrane cholesterol (Fig. 2*F*). Fig. 2 *G* and *H* summarizes the substrate moving between the different secretases based on cluster-associated, apoE-dependent trafficking and the expected cleavage products based on localization. With low cholesterol, apoE moves APP to α-secretase, generating more sAPP-α (Fig. 2 *H*, *Top*). During high cholesterol, apoE moves APP to β- and γ-secretase, which produce Aβ peptide (Fig. 2 *H*, *Bottom*).

The Role of Astrocyte Cholesterol in Regulating APP Processing in Cultured Primary Neurons. Since astrocytes regulate cholesterol levels and cluster formation in neurons (Fig. 1), we hypothesized that astrocytes could directly control Aβ production in neuronal membranes. To test this hypothesis, we cultured primary cortical cells from mouse embryos (E17). In a first culture, we isolated just the neurons by sorting the cells with live cell fluorescence-activated cell sorting (FACS) with Thy1.2, a cell surface marker of mature neurons. In a second culture, we did not remove contaminating astrocytes from neurons, resulting in a mixed culture. All cultures were treated with or without apoE, fixed, and labeled with appropriate fluorophores; the neurons were then imaged with dSTORM. We confirmed the presence of astrocytes in our mixed culture by staining for glial fibrillary acidic protein (GFAP). About 1% of the mixed cell population was labeled by the GFAP antibody (*SI Appendix*, Fig. S3*F*).

We found that the incubation of purified cortical neurons ($Thy1.2^{+}$ with no astrocytes) with cholesterol-free human apoE dramatically decreased APP association with GM1 domains (>twofold) (Fig. 3*B*) in primary neurons. However, when we mixed

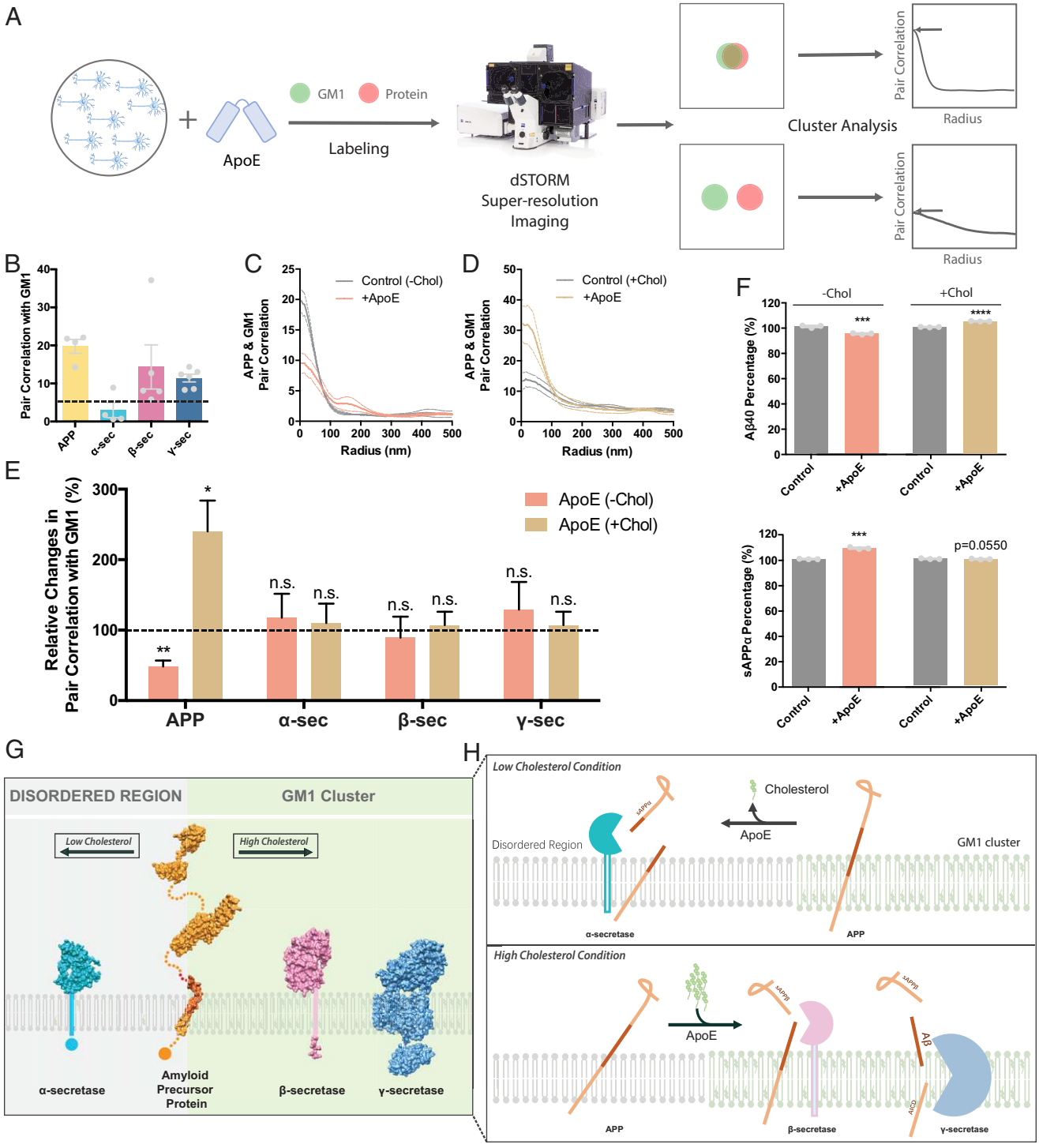

Fig. 2. APP is regulated by cholesterol, not its hydrolytic enzymes. (*A*) Workflow for dSTORM superresolution. Cultured cells (blue) are depicted in a dish. Cells were exposed to apoE with and without cholesterol supplementation and fixed. GM1 lipids and amyloid proteins were fluorescently labeled (CTxB and antibody, respectively) and imaged with superresolution (dSTORM). The proximity of the two labels (shown as red and green circles) was then determined by cluster analysis. Idealized pair correlations are shown for objects that strongly colocalize (*Top*) and weakly colocalize (*Bottom*) at a given radius. Pair correlations are unitless with 1 being little to no correlation and >5 a value typically significant in our experimental conditions. (*B*) α-secretase sits in the disordered region (low correlation with GM1 lipid clusters), while APP, β-, and γ-secretases are GM1 associated in N2a cells. (*C* and *D*) Pair correlation analysis showing that APP moving in (*C*) and out (*D*) of the GM1 clusters under high- and low-cholesterol conditions, respectively. (*E*) Under low-cholesterol conditions (−Chol), APP colocalization with GM1 clusters decreases markedly after apoE treatment. Under high-cholesterol conditions (+Chol), apoE-mediated APP colocalization with GM1 clusters increases (i.e., apoE induces APP to cluster with GM1 lipids). α-, β-, and γ-secretase localization do not respond to apoE-mediated GM1 clustering. (*F*) ELISA in N2a cells showing a shift from Aβ to sAPP-α production after apoE treatment under low-cholesterol condition and increased Aβ production under high-cholesterol condition. Data are expressed as mean ± SEM, $n = 3$ to 10. $^{*}P < 0.05$, $^{**}P < 0.01$, $^{***}P < 0.001$, $^{****}P < 0.0001$, n.s. (not significant), and two-sided Student's *t* test. (*G* and *H*) Because of cluster disruption mediated by apoE, APP is dissociated from GM1 clusters under low-cholesterol conditions, exposing it to α-secretase to be cleaved into nonamyloidogenic sAPP-α. With high, environmental cholesterol, apoE-induced cluster stabilization mediates more APP to be translocated into lipid clusters and cleaved by β- and γ-secretase, producing amyloidogenic Aβ peptides.

astrocytes with neurons, the same apoE had the exact opposite effect. GM1 domains sequestered APP, evident by a 2.5-fold increase in APP association with GM1 lipids (Fig. 3*C*). This suggests that apoE delivers cholesterol from the astrocytes to the neurons and increases GM1 domain affinity for APP. Similar imaging of the secretases showed that they remained immobile with α-secretase in the disordered region and β-secretase in GM1 domains (*SI Appendix*, Fig. S3). Thus, astrocyte-derived cholesterol is a potent signal that controls APP association with α- or β-secretase in the neuron, based on GM1 domain affinity.

To further establish astrocyte-derived cholesterol as the regulator of APP association with secretases, we specifically knocked down cholesterol synthesis in astrocytes by knocking out the SREBP2 gene using a tamoxifen-inducible Cre recombinase system (Fig. 3*A*). SREBP2 is the master transcriptional regulator of the majority of enzymes involved in cholesterol synthesis. Mice with SREBP2 knocked out of astrocytes have reduced the production of cholesterol in the astrocytes (47) (*SI Appendix*, Fig. S4*A*). We cultured cortical neurons and astrocytes from E17 pups and treated them with 100 nM 4-hydroxytamoxifen for 2 d to induce knockout of astrocyte SREBP2. Around 3 d after 4-hydroxytamoxifen removal, the cells were fixed and labeled, and APP localization was imaged with dSTORM, identical to the FACS-sorted neurons above (see diagrams in Fig. 3).

Fig. 3*D* shows a highly significant decrease in APP pair correlation with GM1 domains in mixed cultures containing SREBP2 ($^{-/-}$) astrocytes, similar to purified Thy1.2^{+} neuronal cultures (Fig. 3*B*). Control cells from Thy1.2^{+} neurons and SREBP2 ($^{-/-}$) neuron/astrocyte cultures were very similar; the amplitude of pair correlation was ∼10 for both cultures. 4-hydroxytamoxifen treatment did not significantly alter APP GM1 pair correlation in the absence of Cre recombinase (*SI Appendix*, Fig. S4*B*).

We next examined if astrocytes contribute cholesterol to promote APP presence in neuronal lipid clusters in vivo. Astrocyte cholesterol synthesis was disrupted in mice by crossing SREBP2 floxed mice to GFAP-Cre mice, resulting in a homozygous deletion of SREBP2 from astrocytes (47). At 4 wk of age, brains were collected, and APP-GM1 pair correlation was determined in neurons by dSTORM imaging. SREBP2 deletion in astrocytes resulted in a robust and significant reduction of APP-GM1 pair correlation compared to littermate controls (Fig. 3*E*). This suggests that astrocyte cholesterol synthesis plays an essential role in maintaining cholesterol content in neuronal lipid clusters. These data further confirmed that astrocyte-derived cholesterol regulates APP translocation and association with secretases in the plasma membrane of neurons. Neurons appear incapable of increasing cholesterol synthesis to compensate for astrocyte deficiency in any appreciable way (48).

The In Vivo Role of Astrocyte Cholesterol on Aβ and Plaque Formation in Mouse Brain. Cholesterol is high in AD brains (1, 6). Our model predicts that the attenuation of cholesterol in astrocytes should reduce the concentration of Aβ peptide formed in vivo. To test this hypothesis and to investigate the effect of astrocyte cholesterol on Aβ plaque formation in the intact brain, we crossed 3xTg-AD mice, a well-established mouse model with AD pathology (49), with our SREBP2$^{flox/flox}$ GFAP–Cre mice (47) to generate an AD mouse model lacking astrocyte cholesterol. In vivo Aβ exists in several forms, with Aβ1 to Aβ40 being the most abundant and Aβ1 to Aβ42 the most closely associated with AD pathology. The 3xTg-AD mouse expresses transgenes for mutant human APP and mutant presenilin 1 enzyme, resulting in a significant increase in human Aβ40 and Aβ42 production.

Using ELISAs, we measured human APP transgene-derived Aβ40 and Aβ42 in both the radioimmunoprecipitation assay buffer (RIPA) –soluble and –insoluble fractions in the hippocampus of aged control and transgenic AD mice. Hippocampus tissue from WT control mice was assessed to determine the nonspecific background of the Aβ signal in each ELISA. Knockout of SREBP2 in astrocytes of 3xTg-AD mice (AD × SB2$^{-/-}$) reduced soluble Aβ40 and Aβ42 levels in the hippocampus of 60-wk-old mice by twofold, to levels only slightly higher than WT controls (Fig. 4*A*), suggesting a near complete loss of amyloidogenic processing of APP. More impressively, insoluble Aβ40 and Aβ42 were almost entirely eliminated from the AD × SB2$^{-/-}$ hippocampus (Fig. 4*A*). This was verified by immunofluorescence staining demonstrating an absence of amyloid plaques in AD × SB2$^{-/-}$ mice (Fig. 4*B*). Of note, total APP transgene expression was not impacted by the loss of astrocyte SREBP2 (*SI Appendix*, Fig. S6*A*). Additionally, total GFAP and ApoE protein levels were not significantly changed by SREBP2 ablation (*SI Appendix*, Fig. S6*B*). To further confirm that the reduced Aβ plaque burden in our model was due to reduced amyloidogenic processing, we performed mixed primary cultures of astrocytes and neurons from these 3xTg crosses. In agreement with our in vivo observation, we found that astrocyte SREBP2 deletion modestly increased sAPP-α production and robustly reduced sAPP-β generation without changing total APP abundance (Fig. 5 *A*–*C*). The 3xTg-AD model also expresses a transgene for human tau protein, another key component of Alzheimer's pathology. Tau is hyperphosphorylated in AD, and this is thought to be downstream of Aβ accumulation (50). It has also been proposed that cholesterol directly regulates tau phosphorylation (51, 52). In agreement with both of these hypotheses, phosphorylation of tau at the key T181 residue, but not total tau, is eliminated in vivo in the AD × SB2$^{-/-}$ hippocampus and reduced in mixed cultures in vitro (Figs. 4 *C* and *D* and 5*C* and *SI Appendix*, Fig. S6*A*). We also observed reduced brain tissue volume in AD × SB2$^{-/-}$ animals, similar to that of astrocyte-specific SB2$^{-/-}$ mouse brains characterized in our previous studies (47).

The Role of Astrocytic apoE in Regulating Membrane Cholesterol. Although apoE is the major cholesterol transport protein in the brain, there are other proteins that may also contribute significantly to cholesterol transportation in the central nervous system. To test the effect of astrocytic apoE in transporting cholesterol, we treated neurons with astrocyte-conditioned media (ACM) from APOE knockout mice and compared the cholesterol loading effect with neurons treated with WT ACM (Fig. 6*A*). Specifically, we cultured neurons from SREBP2 GFAP–Cre mice to eliminate the transport of cholesterol from contaminating astrocytes in the culture. Neurons were treated with neurobasal media conditioned with astrocytes from WT or APOE$^{-/-}$ animals. In Western blot, we verified that APOE$^{-/-}$ ACM contains no apoE, while WT ACM does (*SI Appendix*, Fig. S7). Compared with control neurons without ACM treatment, WT ACM significantly increased APP's association with GM1 clusters, while APOE$^{-/-}$ ACM did not show any effect (Fig. 6*B*). This result again confirms that astrocytic apoE is required for cholesterol transportation from astrocytes to neurons. Other cholesterol transport proteins in the brain may allow some delivery of cholesterol, but apoE is the major protein for transporting cholesterol into neurons under these culture conditions.

Isoform Specificity of ApoE. As mentioned, the apoE4 isoform is a strong genetic risk factor for late onset AD. If this effect is in part through cholesterol loading, we would expect to see a difference in APP's submembrane localization. To study the difference between apoE3 and apoE4 in vivo, we analyzed the brain tissue from APOE knock in (KI) mice, in which the human APOE variants (ε3 and ε4) replace the endogenous murine Apoe locus (termed E3F and E4F mice individually). We assessed these mice both alone and after crossing them with mice with amyloid deposition in the brain by crossing the different APOE-KI mice with APP/PS1 transgenic mice. We found that an increased association of APP with GM1 lipids in E4F compared to E3F (Fig. 6*C*). Interestingly, overexpression of mutant APP and mutant PS1 (APP/PS1) with resulting amyloid deposition has an even more dramatic effect

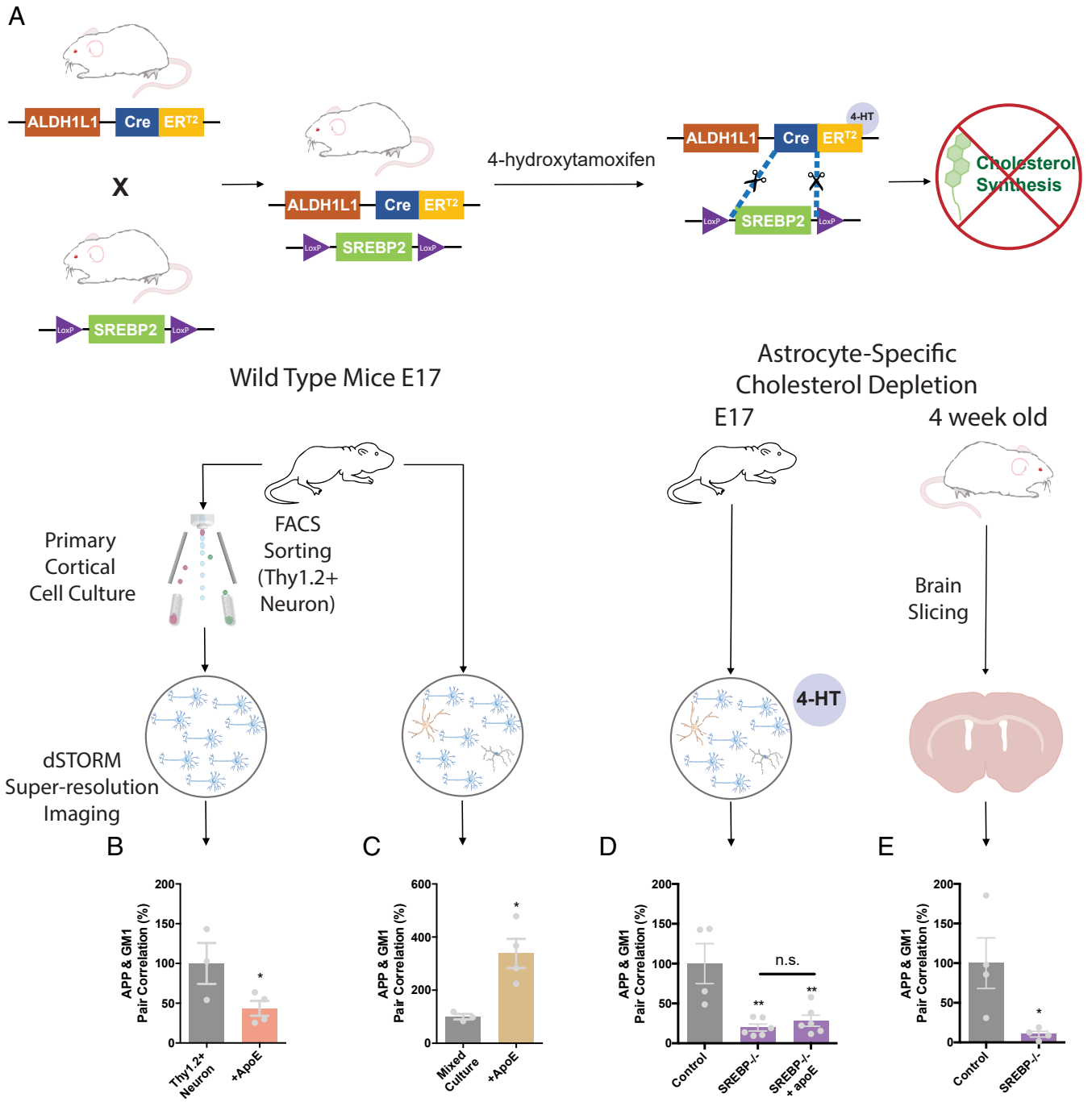

Fig. 3. Astrocyte cholesterol regulates APP processing in neurons. (*A*) Strategy for conditional knockout of SREBP2 in astrocytes using Cre-Lox recombination system. SREBP2 flox mice were crossed to ALDH1L1-specific Cre transgenic mice, which express Cre recombinase specifically in astrocytes when presented 4-hydroxytamoxifen (4-HT). Cre promotes SREBP2 knockout and blocks cholesterol synthesis in astrocytes. (*B–D*) Cortical cells were isolated from embryonic day 17 mice and cultured for dSTORM imaging. (*B*) ApoE translocates APP from lipid clusters into disordered regions in a pure, neuronal population sorted with cell surface neuronal marker Thy1.2. (*C*) ApoE increases APP's cluster localization in primary neurons cultured in mixed population with glia cells, including astrocytes. (*D*) Astrocyte-specific cholesterol depletion completely disrupts APP cluster localization in neurons in cultured cells. (*E*) Astrocyte cholesterol depletion disrupts APP cluster localization in vivo, as demonstrated in SREBP2$^{fl/fl}$ GFAP–Cre$^{+/-}$ mouse brain slices. Data are expressed as mean ± SEM, $n = 3$ to 10, $^{*}P < 0.05$, $^{**}P < 0.01$, one-way ANOVA (*D*), or two-sided Student's *t* test (*B*, *C*, and *E*).

than APOE genotype. Brain tissue from APP/PS1 mice has significantly increased APP-GM1 association (Fig. 6*C*). We also measured the tissue cholesterol level of the brains and observed a similar trend, as we found in APP-GM1 pair correlation. Though not statistically significant, the E4F brains have a slightly higher cholesterol level than E3F brains (Fig. 6*D*). Similarly, the APP/PS1/E4F brains have a slightly higher cholesterol level than APP/PS1/E3F brains (Fig. 6*D*). APP/PS1 overexpression robustly increases brain tissue cholesterol level (Fig. 6*D*).

Lastly, we tested the effect of purified apoE3 or apoE4 proteins to selectively transport cholesterol. We incubated N2a cells with purified apoE proteins with or without cholesterol exposure

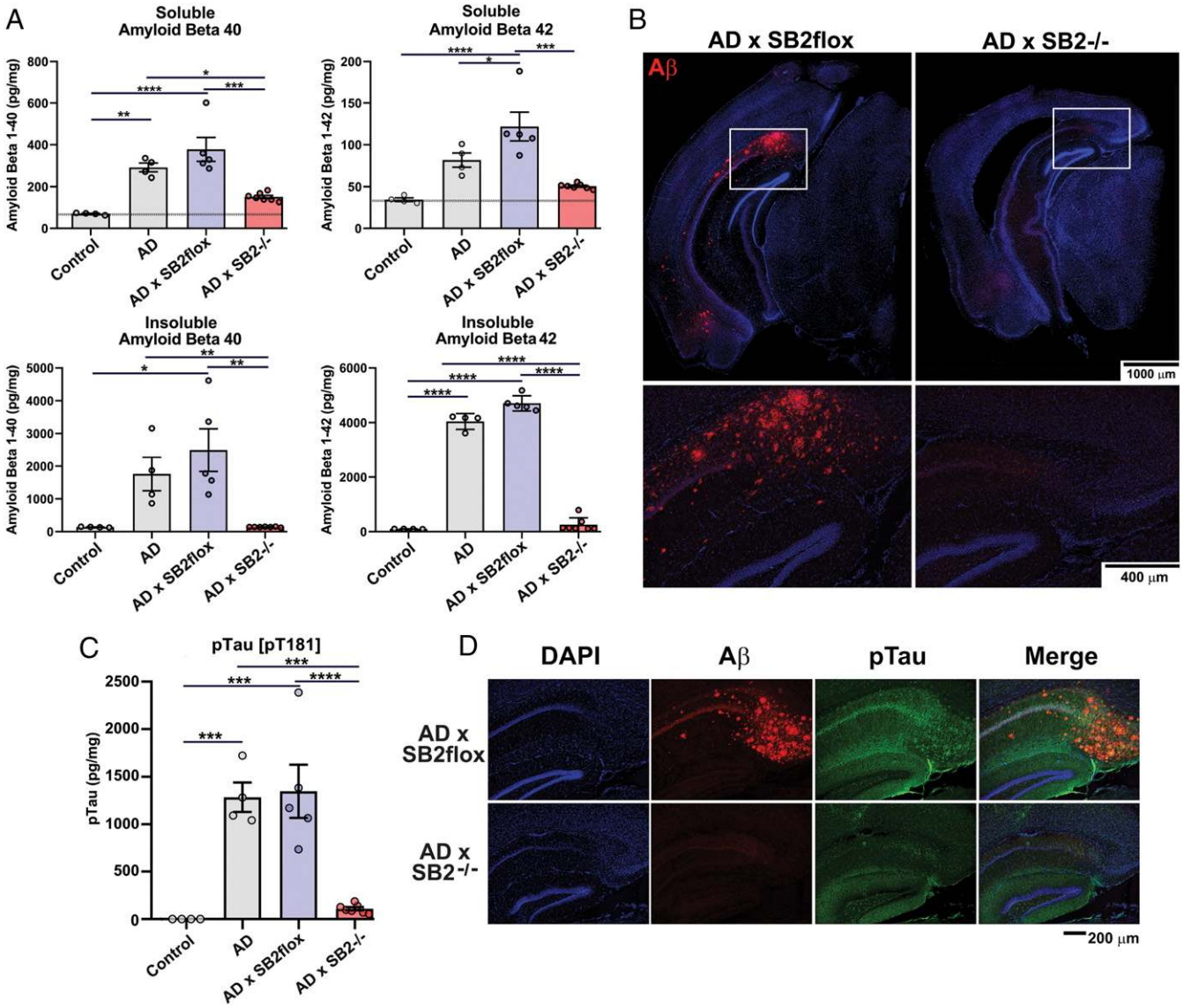

Fig. 4. Loss of cholesterol synthesis in astrocytes blocks Aβ plaque formation and Tau phosphorylation in vivo. 3xTg-AD mice (AD) were crossed to SREBP2$^{fl/fl}$ GFAP–Cre$^{+/-}$ mice (AD × SB2$^{-/-}$) and aged to 60 wk. (*A*) Hippocampus were isolated and soluble (RIPA extracted) and insoluble (guanidine extracted) Aβ40 and Aβ42 species were measured by ELISA. (*B*) 60-wk-old brain slices stained for human Aβ (red) and DAPI (blue) in AD × SB2flox mice (*Left*) and AD × SB2$^{-/-}$ mice (*Right*). (*C*) pTau levels were measured in 60-wk-old hippocampus lysate by ELISA. (*D*) 60-wk-old brain slices were immune stained for pTau (green) and Aβ (red), and the subiculum region of the hippocampus was imaged. Data are expressed as mean ± SEM, $n = 4$ to 7, one-way ANOVA with Tukey's post hoc analysis, $^{*}P < 0.05$, $^{**}P < 0.01$, $^{***}P < 0.001$, and $^{****}P < 0.0001$.

(Fig. 6*E*). Under low-cholesterol condition, both apoE3 and apoE4 trafficked APP out of GM1 clusters into disordered regions, with no significant difference between the two isoforms (Fig. 6*F*). Similarly, when exposed to high cholesterol, apoE3 and apoE4 increase APP's cluster association with no significant difference between isoforms (Fig. 6*G*). We also measured cellular cholesterol level after cholesterol extraction by apoE3 and apoE4. Total cholesterol level decreased after apoE incubation. We didn't observe any difference between the two isoforms (Fig. 6*H*). The results indicate that the difference in the in vivo regulation is not a functional difference in the efficiency of an isoform to transport cholesterol.

Discussion

Together, our data support astrocyte cholesterol as a key regulator of neuronal Aβ accumulation. The data from cultured neurons and astrocytes show that astrocyte-secreted apoE loads cholesterol into neurons. Increased cholesterol in neurons drives APP to associate with β- and γ-secretases in lipid clusters. The association of APP with lipid clusters appears to regulate the amount of Aβ accumulation, and Aβ levels dictate insoluble plaques (Fig. 7).

While it has been known for some time that astrocytes play an important role in brain cholesterol production and express the AD-related protein apoE, the role of astrocytes in AD pathogenesis remains poorly understood (53–55). Astrocytes undergo robust morphological changes in neurodegenerative models, and recent research demonstrates that astrocytes undergo broad transcriptional changes early in the AD process (56). However, whether astrocytes are simply reacting to the AD neurodegenerative cascade or playing a role in promoting disease remains unclear. Here, we demonstrate a direct role for astrocytes in promoting the AD phenotype through the production and distribution of cholesterol to neurons. Combined, our data establish

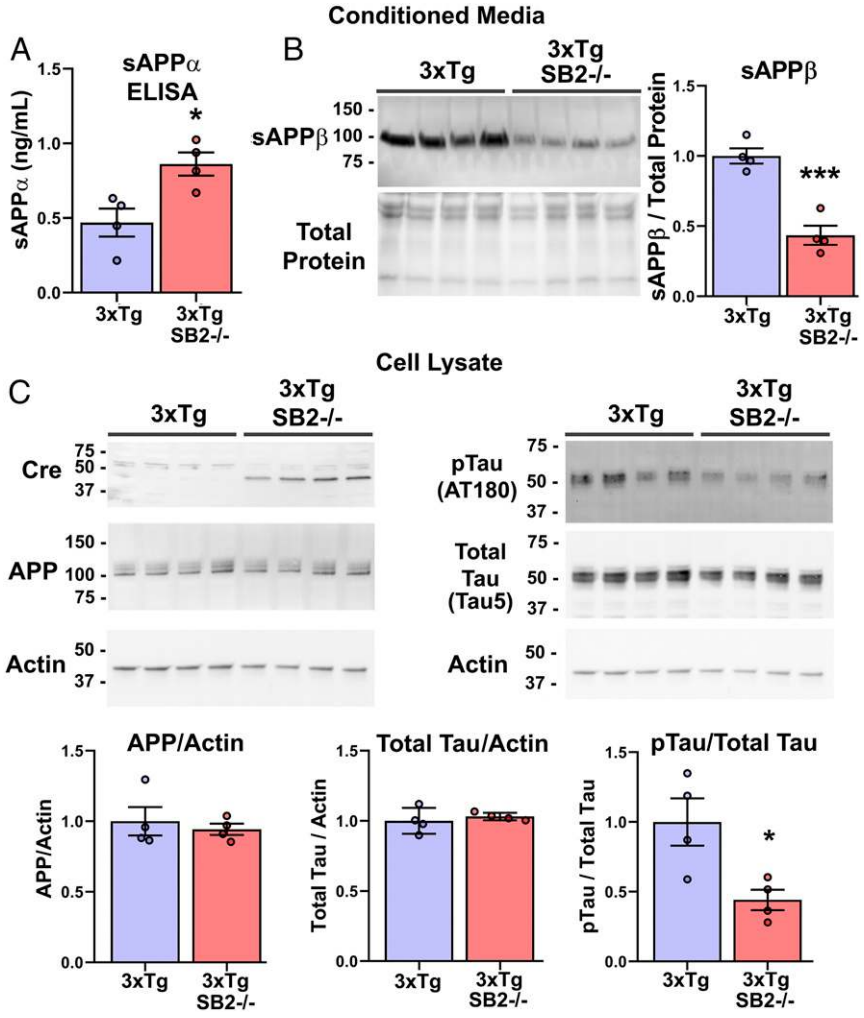

Fig. 5. Astrocyte cholesterol regulates APP and Tau processing, not protein expression. Primary embryonic cultures of mixed neurons and astrocytes were grown by crossing 3xTg SREBP2$^{fl/fl}$ mice with 3xTg SREBP2$^{fl/fl}$ GFAP–Cre mice. Each culture was grown independently from a single embryo, and Cre genotype was confirmed by PCR. (*A*) Human sAPP-α levels (from transgenic APP) were measured in conditioned media from mixed cultures. (*B*) Protein in conditioned media was precipitated, and sAPP-β, an APP fragment produced by β-secretase cleavage, was measured by Western blot. (*C*) Mixed cultures were lysed, and protein content was examined by Western blot. Data are expressed as mean ± SEM and $n = 4$ per genotype. $^*P < 0.05$ and $^{***}P < 0.001$.

a molecular pathway that connects astrocyte cholesterol synthesis with apoE lipid trafficking and amyloidogenic processing of APP (Fig. 7). The pathway establishes cholesterol as a critical lipid that controls the signaling state of a neuron. Cholesterol appears to be down-regulated in neurons as part of a mechanism to allow astrocytes to control APP presentation to proteolytic enzymes in the neuron. By keeping cholesterol low, the astrocyte can move the neuron through a concentration gradient that profoundly affects APP processing and eventual plaque formation. In essence, cholesterol is set up to be used as a signaling lipid. Rather than targeting a receptor, it targets GM1 domains and sets the threshold for APP processing by altering GM1 domain function. This concept is likely important to other biological systems (57), given the profound effect of cholesterol on human health.

The rise and fall of Aβ peptide with cholesterol is striking (Fig. 4 *A* and *B*), and the data presented here support the proposed molecular mechanism in which amyloidogenic processing of APP is promoted by cholesterol increasing APP interactions with β- and γ-secretases through substrate presentation (*SI Appendix*, Fig. S1). This finding is in agreement with prior research, implicating increased brain cholesterol content as a factor which promotes AD-associated amyloid pathology. Administration of statins to guinea pigs significantly reduces Aβ levels in the cerebrospinal fluid (58), and statins reduced β secretase processing in induced pluripotent stem cell (iPSC) –derived neurons (59). APP/PS1 AD mice overexpressing a truncated active form of SREBP2 display an accelerated Aβ burden with aging (60). The conclusion is further supported by the existence of a cholesterol binding site in the APP protein (61). Our findings contribute to literature, demonstrating that amyloidogenic processing of APP in cultured cells occurs primarily in cholesterol-rich membrane domains (15, 62) and is consistent with cholesterol unloading decreasing Aβ formation in cell culture (63) and on the plasma membrane (64).

Several lines of evidence suggest that cholesterol and its trafficking by lipoprotein particles also influences hyperphosphorylation of tau in neurons. van der Kant et al. found that, by disrupting cholesterol production using statins or enhancing cholesterol clearance, both pTau and total tau levels were reduced in cultured iPSC neurons (51). Interestingly, statins had no effect on neuronal pTau levels in the presence of proteasome inhibitors, suggesting that high levels of cholesterol in neurons may slow the intracellular clearance of tau protein. Moreover, we recently demonstrated that deletion of astrocyte apoE in a mouse model of tauopathy mitigates

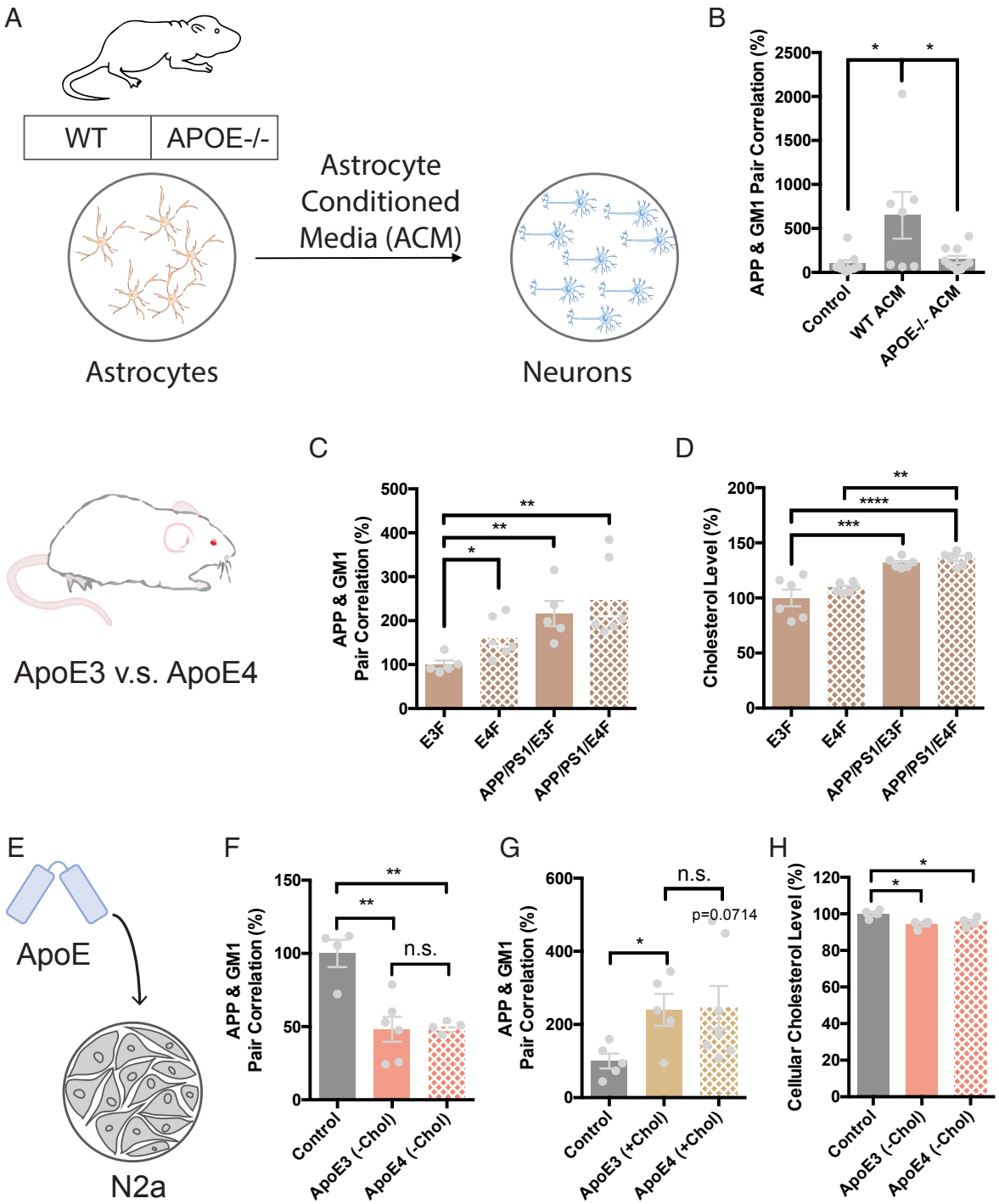

Fig. 6. Astrocytic apoE is required for cholesterol transportation from astrocytes to neurons. (*A*) Cartoon diagram showing the experimental setup for neuron culture with ACM. Neurons from SREBP2 GFAP–Cre mice were used to eliminate transport of cholesterol from contaminating astrocytes in the culture. Neurons were cultured with ACM from either WT or APOE$^{-/-}$ astrocytes. (*B*) dSTORM superresolution imaging shows that astrocytic apoE is required for regulating APP's GM1 clustering in neurons. Neurons cultured with ACM-containing apoE increased APP's clustering with GM1 lipids, while ACM from APOE$^{-/-}$ animals fail to increase APP's cluster association. (*C*) APP in APOE4 brains (E4F) are more clustered with GM1 lipids, compared with E3F. Aβ overexpression (APP/PS1) also robustly increases APP's raft association. APP/PS1/E4F has slightly higher APP-GM1 pair correlation than APP/PS1/E3F. (*D*) Aβ overexpression (APP/PS1) increases brain cholesterol level robustly. In both control and APP/PS1 animals, E4F has a slightly higher cholesterol level in brain tissue compared with E3F. Data are expressed as mean ± SEM, $n = 3$ to 10, $^{*}P < 0.05$, $^{**}P < 0.01$, $^{***}P < 0.001$, $^{****}P < 0.0001$, and one-way ANOVA. (*E*) N2a cells were treated with purified apoE3 or apoE4 proteins to compare their abilities to load and unload cholesterol (± Chol) from the plasma membrane. (*F*) Under low-cholesterol condition, apoE extracts cholesterol from the cells, decreasing APP's GM1 clustering. There is no significant difference between apoE3 and apoE4. (*G*) Under high-cholesterol condition, apoE loads cholesterol into the cells, increasing APP's GM1 clustering. There is no significant difference between apoE3 and apoE4. (*H*) Exposure of N2a cells to apoE removes cholesterol from cellular membranes, as measured by a fluorescent-based live cell cholesterol assay. There is no significant difference between apoE3 and apoE4.

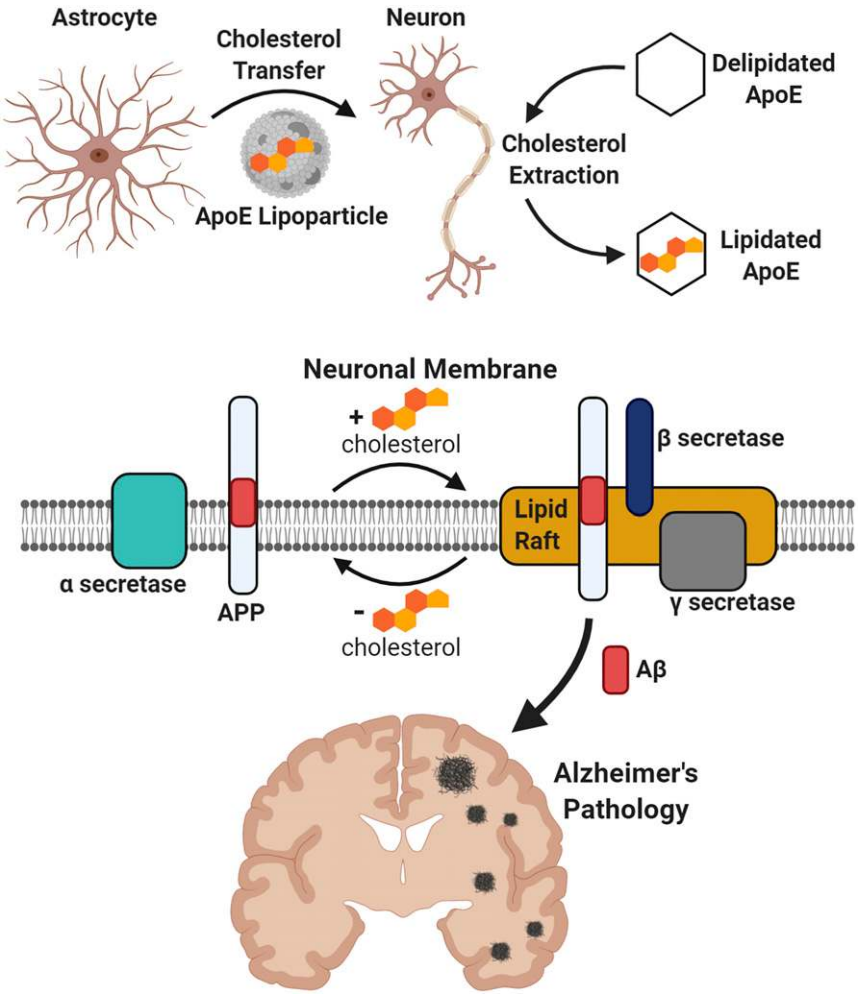

Fig. 7. Astrocyte cholesterol-dependent regulation of amyloid processing in neurons through apoE. A model for amyloid production in the Alzheimer's brain. Cholesterol is synthesized in astrocytes and shuttled to neurons in apoE lipoprotein particles. Adding recombinant, cholesterol-containing apoE enriches neuronal membrane cholesterol levels, while delipidated apoE reduces membrane cholesterol. Cholesterol loading of the neuronal membranes regulates Aβ production by increasing APP interactions with β- and γ-secretase. In low-cholesterol membranes, APP interacts with α-secretase, generating sAPPα. When neuronal membranes are loaded with cholesterol, APP increasingly interacts with β- and γ-secretases generating Aβ peptides, resulting in brain plaque formation over time.

pTau pathology, neurodegeneration, and synapse loss, though total tau levels remained unchanged (65). This could indicate that distinct mechanisms exist for both exogenous and endogenous sources of cholesterol in promoting pTau accumulation in neurons. In a large study of Alzheimer's pathology, APOE variants were shown to have strong effects on tau tangle burden, with APOE4/E4 carriers most adversely affected (66). Notably, a homozygous carrier of the APOE Christchurch mutation was reported to be resistant to cognitive decline and pTau accumulation, even in the presence of a presenilin 1 mutation and robust amyloid plaque deposition (67). Thus, the reduced levels of pTau we observe when astrocyte SREBP2 is ablated are likely driven by both reduced cholesterol levels as well as the alleviation of amyloid burden, though the exact mechanisms by which astrocyte cholesterol influences neuronal tau phosphorylation require future investigations.

The trend toward increased levels of cholesterol in apoE4 KI mice and the increased APP/GM1 clustering are consistent with the increased cholesterol in familial AD patients, which leads to the clustering of APP with lipid rafts (14) and the increased Aβ production seen in neurons expressing apoE4 isoforms (68). We saw no difference on the ability of purified apoE3 and apoE4 to load or unload cholesterol into cultured cells (Fig. 6 *F*–*H*); we conclude that cellular regulation of apoE, or protein abundance, is likely responsible apoE's isoform-specific effects in vivo.

Cholesterol loading into glial cells is known to cluster inflammatory proteins and cause inflammation (69); hence, cholesterol in APP regulation suggests a correlative link between inflammation in AD and Aβ production. A previous study found gene expression–controlled Aβ production (70). We saw dramatic changes in Aβ production without any appreciable change to APP expression levels (Fig. 5). Nonetheless, the two mechanisms are not mutually exclusive, and increased APP expression would be synergistic with increased cutting in response to high cholesterol.

At the molecular level, cholesterol loading regulates two functions: 1) the localization of APP to GM1 domains and 2) the total number of GM1 domains (Fig. 1 *D* and *E*). Palmitoylation drives the cluster association of the majority of integral cluster proteins (7), but β- and γ-secretases are also palmitoylated and remain localized to GM1 lipids, suggesting a difference in relative affinity or additional factors that facilitate its release from GM1 domains [e.g., hydrophobic mismatch (71)].

Many channels are palmitoylated (72) and may respond to apoE and GM1 lipid domain function similar to APP. Investigating the effect of astrocyte cholesterol on channels will be important for studying AD, since many of the palmitoylated channels

have profound effects on neuronal excitability and learning and memory (72). In separate studies, we saw that cholesterol loading with apoE caused the potassium channel TREK-1 to traffic to lipid clusters similar to APP (73, 74)—an effect that was reversed by mechanical force (75).

Our data suggest cultured cells lacking apoE supplementation likely underestimate physiological GM1 domain size, especially those derived from the brain where cholesterol is high (76). Not surprisingly, clusters appeared to be absent in cultured cells (77). Not until cholesterol, supplied by astrocytes or cholesterol-containing apoE, was added were nanoscale clusters present (~100 nm). We conclude from our data that the conditions with cholesterol are the more physiologically relevant conditions for cultured cells.

All astrocyte-targeting Cre lines also delete to some degree in neural progenitor cells. While our model also suffers from this shortcoming, we have previously demonstrated that overall cholesterol synthesis by neurons increases to compensate for the loss of astrocyte cholesterol (47). Thus, the dramatic decrease in Aβ and pTau that we observe in our AD × SB2($^{-/-}$) mice cannot readily be explained by the minority of knocked out neurons. In addition, microglia, which are also able to produce apoE (47) and are not impacted by the Cre, are unable to compensate for a lack of astrocyte cholesterol synthesis. Our data emphasize that the small changes in Aβ production we see in our cell culture models may have a meaningful impact in vivo, such that the cumulative impact of altering cholesterol delivery to neurons can be observed.

We conclude that the availability of astrocyte cholesterol regulates Aβ production by substrate presentation. This contributes to the understanding of AD and provides a potential explanation for the role of cholesterol-associated genes as risk factors for AD.

Materials and Methods

Cell Cultures. The primary neurons, embryonic day 17 brain cortices, were harvested from embryos and cultured with neurobasal medium supplemented with 20% B27, 1% Glutamax, and 1% penicillin/streptomycin, while tails from each individual embryo were collected for the determination of Cre genotype. Astrocytes, N2a, and human embryonic kidney 293T cells were grown in standard Dulbecco's Modified Eagle Medium with 10% FBS.

dSTORM.

Fixed cells. Cells were incubated with 4 μg/mL purified apoE protein for 1 h in media with or without 10% FBS supplementation and then fixed with 3% paraformaldehyde and 0.1% glutaraldehyde for 15 min. Cells were permeabilized with 0.2% Triton X-100 for 15 min and then blocked with 10% bovine serum albumin (BSA)/0.05% Triton in phosphate-buffered saline (PBS) for 90 min at room temperature. Cells were labeled with primary antibody for 60 min and secondary antibody for 30 min at room temperature with blocking then fixed again. We note that the anti-APP antibody (ab15272) used for dSTORM was different from the anti-APP antibody (ab32136) used for Western blots. Both antibodies were previously validated; see *SI Appendix, Extended Methods* for a complete description of all the antibodies and their validation used for imaging.

Brain slices. Mouse brain was fixed in 4% paraformaldehyde and 20% sucrose/PBS solution at 4 °C for 3 d and embedded in Tissue-Tek optimal cutting temperature (OCT) compound (Sakura) and sliced sagittal (50 μm). Primary and secondary antibodies were incubated for 3 d each with washing in between and postfixation. Brain slices were mounted onto the 35-mm glass bottom chamber (ibidi, No. 81158) with 2% agarose to form a permeable agarose pad and prevent sample movement during imaging.

Amyloid and pTau ELISAs.

Cell cultures. Supernatants from cells or brain tissue were analyzed for the presence of Aβ40 and sAPP-α with a commercial human Aβ40 ELISA kit (Invitrogen, #KHB3481) following the manufacturer's instructions or anti-rabbit APP antibody abcam, #ab15272. Human Aβ1 to Aβ40 (R&D Systems, #DAB140B) and Aβ1 to Aβ42 (R&D Systems, #DAB142) were quantified in mouse hippocampus tissue using commercially available ELISA kits per manufacturer's instructions. Whole hippocampus tissue was homogenized from 60-wk-old female mice in RIPA buffer (Bioworld, #42020024–2) with protease inhibitors.

Western Blots. The 40-wk-old mouse hippocampus tissue was homogenized in RIPA buffer with protease inhibitors and run on sodium dodecyl sulfate–polyacrylamide gel electrophoresis. Resolved protein was transferred to polyvinylidene difluoride membrane and blocked with a 5% BSA solution in PBS with Tween 20. Primary antibodies against target proteins were applied overnight at 4 °C and imaged with a fluorescent secondary antibody.

Lipidomics. Lipidomics profiling was performed using ultra-performance liquid chromatography–tandem mass spectrometry by core services available from Columbia University.

Statistics. All statistical calculations were performed in GraphPad Prism version 6.0. For the Student's *t* test, significance was calculated using a two-tailed, unpaired parametric test with significance defined as $*P < 0.05$, $**P < 0.01$, $***P < 0.001$, and $****P < 0.0001$. For the multiple comparison test, significance was calculated using an ordinary one-way ANOVA with Dunnett's multiple comparisons test.

Data Availability. dSTORM and biochemical assay data have been deposited in Mendeley (https://doi.org/10.17632/4s373hyhj6.1) (78). All other study data are included in the article and/or supporting information.

ACKNOWLEDGMENTS. We thank Andrew S. Hansen and Damon Page for the aspects of experimental design, E. Nicholas Petersen for his help and discussion on the imaging and imaging analysis, and Eddie Grinman and the Puthanveettil laboratory for mouse cortical tissue. We thank the biomarker core (Columbia University) and flow cytometry core (Scripps Research) for technical support. We thank Kai Simons, Stuart Lipton, Lawrence Goldstein, Shannon Macauley-Rambach, and Lance Johnson for their helpful discussion and reading of the manuscript. This work was supported by the NIH via a Director's New Innovator Award to S.B.H. (DP2NS087943), R01 to S.B.H. (Grant R01NS112534), K08 (Grant K08DK097293) and Owens Family Foundation Award to H.A.F., NIH T32 (Grant T32DK764627) to J.A.K., and NIH Grants NS090934 and AG047644 to D.M.H. We are grateful to The JPB Foundation for the purchase of a superresolution microscope.

1. C. Haass, D. J. Selkoe, Cellular processing of β-amyloid precursor protein and the genesis of amyloid β-peptide. *Cell* **75**, 1039–1042 (1993).
2. E. Shokri-Kojori *et al.*, β-amyloid accumulation in the human brain after one night of sleep deprivation. *Proc. Natl. Acad. Sci. U.S.A.* **115**, 4483–4488 (2018).
3. L. Xie *et al.*, Sleep drives metabolite clearance from the adult brain. *Science* **342**, 373–377 (2013).
4. M. L. Gosztyla, H. M. Brothers, S. R. Robinson, Alzheimer's amyloid-β is an antimicrobial peptide: A review of the evidence. *J. Alzheimers Dis.* **62**, 1495–1506 (2018).
5. Rice, H. C. *et al*. Secreted amyloid-B precursor protein functions as a GABA B R1a ligand to modulate synaptic transmission. *Science* **363**, eaao4827 (2019).
6. M.-P. Marzolo, G. Bu, Lipoprotein receptors and cholesterol in APP trafficking and proteolytic processing, implications for Alzheimer's disease. *Semin. Cell Dev. Biol.* **20**, 191–200 (2009).
7. I. Levental, D. Lingwood, M. Grzybek, U. Coskun, K. Simons, Palmitoylation regulates raft affinity for the majority of integral raft proteins. *Proc. Natl. Acad. Sci. U.S.A.* **107**, 22050–22054 (2010).
8. K. S. Vetrivel, G. Thinakaran, Membrane rafts in Alzheimer's disease beta-amyloid production. *Biochim. Biophys. Acta* **1801**, 860–867 (2010).
9. W. Araki, Post-translational regulation of the β-secretase BACE1. *Brain Res. Bull.* **126**, 170–177 (2016).
10. R. Bhattacharyya, C. Barren, D. M. Kovacs, Palmitoylation of amyloid precursor protein regulates amyloidogenic processing in lipid rafts. *J. Neurosci.* **33**, 11169–11183 (2013).
11. J. M. Cordy, N. M. Hooper, A. J. Turner, The involvement of lipid rafts in Alzheimer's disease. *Mol. Membr. Biol.* **23**, 111–122 (2006).
12. K. S. Vetrivel *et al.*, Alzheimer disease Abeta production in the absence of S-palmitoylation-dependent targeting of BACE1 to lipid rafts. *J. Biol. Chem.* **284**, 3793–3803 (2009).
13. H. Cheng *et al.*, S-palmitoylation of γ-secretase subunits nicastrin and APH-1. *J. Biol. Chem.* **284**, 1373–1384 (2009).
14. Y. Y. Cho, O.-H. Kwon, M. K. Park, T.-W. Kim, S. Chung, Elevated cellular cholesterol in familial Alzheimer's presenilin 1 mutation is associated with lipid raft localization of β-amyloid precursor protein. *PLoS One* **14**, e0210535 (2019).
15. R. Ehehalt, P. Keller, C. Haass, C. Thiele, K. Simons, Amyloidogenic processing of the Alzheimer β-amyloid precursor protein depends on lipid rafts. *J. Cell Biol.* **160**, 113–123 (2003).
16. C. V. Robinson, T. Rohacs, S. B. Hansen, Tools for understanding nanoscale lipid regulation of ion channels. *Trends Biochem. Sci.* **44**, 795–806 (2019).

17. M. A. Pavel, E. N. Petersen, H. Wang, R. A. Lerner, S. B. Hansen, Studies on the mechanism of general anesthesia. *Proc. Natl. Acad. Sci. U.S.A.* **117**, 13757–13766 (2020).
18. E. N. Petersen, H.-W. Chung, A. Nayebosadri, S. B. Hansen, Kinetic disruption of lipid rafts is a mechanosensor for phospholipase D. *Nat. Commun.* **7**, 13873 (2016).
19. G. Di Paolo, T.-W. Kim, Linking lipids to Alzheimer's disease: Cholesterol and beyond. *Nat. Rev. Neurosci.* **12**, 284–296 (2011).
20. C. Reitz, Dyslipidemia and dementia: Current epidemiology, genetic evidence, and mechanisms behind the associations. *J. Alzheimers Dis.* **30** (suppl. 2), S127–S145 (2012).
21. P. Gamba *et al*., The link between altered cholesterol metabolism and Alzheimer's disease. *Ann. N. Y. Acad. Sci.* **1259**, 54–64 (2012).
22. J. Zhao *et al*., β-secretase processing of the β-amyloid precursor protein in transgenic mice is efficient in neurons but inefficient in astrocytes. *J. Biol. Chem.* **271**, 31407–31411 (1996).
23. M. E. Calhoun *et al*., Neuronal overexpression of mutant amyloid precursor protein results in prominent deposition of cerebrovascular amyloid. *Proc. Natl. Acad. Sci. U.S.A.* **96**, 14088–14093 (1999).
24. G. Quan, C. Xie, J. M. Dietschy, S. D. Turley, Ontogenesis and regulation of cholesterol metabolism in the central nervous system of the mouse. *Brain Res. Dev. Brain Res.* **146**, 87–98 (2003).
25. J. M. Dietschy, S. D. Turley, Thematic review series: Brain lipids. Cholesterol metabolism in the central nervous system during early development and in the mature animal. *J. Lipid Res.* **45**, 1375–1397 (2004).
26. D. W. Russell, R. W. Halford, D. M. O. Ramirez, R. Shah, T. Kotti, Cholesterol 24-hydroxylase: An enzyme of cholesterol turnover in the brain. *Annu. Rev. Biochem.* **78**, 1017–1040 (2009).
27. J. E. Vance, H. Hayashi, Formation and function of apolipoprotein E-containing lipoproteins in the nervous system. *Biochim. Biophys. Acta* **1801**, 806–818 (2010).
28. W. J. Strittmatter *et al*., Apolipoprotein E: High-avidity binding to β-amyloid and increased frequency of type 4 allele in late-onset familial Alzheimer disease. *Proc. Natl. Acad. Sci. U.S.A.* **90**, 1977–1981 (1993).
29. Corder, E. H. *et al*. Gene dose of apolipoprotein E type 4 allele and the risk of Alzheimer's disease in late onset families. *Science* **261**, 921–923 (1993).
30. D. Lingwood, K. Simons, Lipid rafts as a membrane-organizing principle. *Science* **327**, 46–50 (2010).
31. E. Sezgin, I. Levental, S. Mayor, C. Eggeling, The mystery of membrane organization: Composition, regulation and roles of lipid rafts. *Nat. Rev. Mol. Cell Biol.* **18**, 361–374 (2017).
32. G. van den Bogaart *et al*., Membrane protein sequestering by ionic protein-lipid interactions. *Nature* **479**, 552–555 (2011).
33. J. Wang, D. A. Richards, Segregation of PIP2 and PIP3 into distinct nanoscale regions within the plasma membrane. *Biol. Open* **1**, 857–862 (2012).
34. S. A. Jones, S.-H. Shim, J. He, X. Zhuang, Fast, three-dimensional super-resolution imaging of live cells. *Nat. Methods* **8**, 499–508 (2011).
35. B. Huang, W. Wang, M. Bates, X. Zhuang, Three-dimensional super-resolution imaging by stochastic optical reconstruction microscopy. *Science* **319**, 810–813 (2008).
36. E. Betzig *et al*., Imaging intracellular fluorescent proteins at nanometer resolution. *Science* **313**, 1642–1645 (2006).
37. S. T. Hess, T. P. K. K. Girirajan, M. D. Mason, Ultra-high resolution imaging by fluorescence photoactivation localization microscopy. *Biophys. J.* **91**, 4258–4272 (2006).
38. A. Honigmann *et al*., Scanning STED-FCS reveals spatiotemporal heterogeneity of lipid interaction in the plasma membrane of living cells. *Nat. Commun.* **5**, 5412 (2014).
39. X. Hua *et al*., SREBP-2, a second basic-helix-loop-helix-leucine zipper protein that stimulates transcription by binding to a sterol regulatory element. *Proc. Natl. Acad. Sci. U.S.A.* **90**, 11603–11607 (1993).
40. R. Srinivasan *et al*., New transgenic mouse lines for selectively targeting astrocytes and studying calcium signals in astrocyte processes in situ and in vivo. *Neuron* **92**, 1181–1195 (2016).
41. J. Luo, H. Yang, B.-L. Song, Mechanisms and regulation of cholesterol homeostasis. *Nat. Rev. Mol. Cell Biol.* **21**, 225–245 (2020).
42. J. Chen, X. Zhang, H. Kusumo, L. G. Costa, M. Guizzetti, Cholesterol efflux is differentially regulated in neurons and astrocytes: Implications for brain cholesterol homeostasis. *Biochim. Biophys. Acta* **1831**, 263–275 (2013).
43. H. Hayashi, R. B. Campenot, D. E. Vance, J. E. Vance, Apolipoprotein E-containing lipoproteins protect neurons from apoptosis via a signaling pathway involving low-density lipoprotein receptor-related protein-1. *J. Neurosci.* **27**, 1933–1941 (2007).
44. V. P. Varma *et al*., Ocular fluid as a replacement for serum in cell cryopreservation media. *PLoS One* **10**, e0131291 (2015).
45. M. Lindh *et al*., Cerebrospinal fluid apolipoprotein E (apoE) levels in Alzheimer's disease patients are increased at follow up and show a correlation with levels of tau protein. *Neurosci. Lett.* **229**, 85–88 (1997).
46. R. Zidovetzki, I. Levitan, Use of cyclodextrins to manipulate plasma membrane cholesterol content: Evidence, misconceptions and control strategies. *Biochim. Biophys. Acta* **1768**, 1311–1324 (2007).
47. H. A. Ferris *et al*., Loss of astrocyte cholesterol synthesis disrupts neuronal function and alters whole-body metabolism. *Proc. Natl. Acad. Sci. U.S.A.* **114**, 1189–1194 (2017).
48. C.-C. Liu, C.-C. Liu, T. Kanekiyo, H. Xu, G. Bu, Apolipoprotein E and Alzheimer disease: Risk, mechanisms and therapy. *Nat. Rev. Neurol.* **9**, 106–118 (2013).
49. S. Oddo *et al*., Triple-transgenic model of Alzheimer's disease with plaques and tangles: Intracellular Abeta and synaptic dysfunction. *Neuron* **39**, 409–421 (2003).
50. D. J. Selkoe, J. Hardy, The amyloid hypothesis of Alzheimer's disease at 25 years. *EMBO Mol. Med.* **8**, 595–608 (2016).
51. R. van der Kant *et al*., Cholesterol metabolism is a druggable axis that independently regulates tau and amyloid-β in iPSC-derived Alzheimer's disease neurons. *Cell Stem Cell* **24**, 363–375.e9 (2019).
52. R. van der Kant, L. S. B. Goldstein, R. Ossenkoppele, Amyloid-β-independent regulators of tau pathology in Alzheimer disease. *Nat. Rev. Neurosci.* **21**, 21–35 (2020).
53. D. H. Mauch *et al*., CNS synaptogenesis promoted by glia-derived cholesterol. *Science* **294**, 1354–1357 (2001).
54. M. J. LaDu *et al*., Nascent astrocyte particles differ from lipoproteins in CSF. *J. Neurochem.* **70**, 2070–2081 (1998).
55. J. K. Boyles, R. E. Pitas, E. Wilson, R. W. Mahley, J. M. Taylor, Apolipoprotein E associated with astrocytic glia of the central nervous system and with nonmyelinating glia of the peripheral nervous system. *J. Clin. Invest.* **76**, 1501–1513 (1985).
56. N. Habib *et al*., Disease-associated astrocytes in Alzheimer's disease and aging. *Nat. Neurosci.* **23**, 701–706 (2020).
57. H. Wang, Z. Yuan, M. A. Pavel, S. Hansen, The role of high cholesterol in aged related COVID19 lethality. *bioRxiv* [Preprint] (2020). https://www.biorxiv.org/content/10.1101/2020.05.09.086249v5. Accessed 3 August 2021.
58. K. Fassbender *et al*., Simvastatin strongly reduces levels of Alzheimer's disease β -amyloid peptides Abeta 42 and Abeta 40 in vitro and in vivo. *Proc. Natl. Acad. Sci. U.S.A.* **98**, 5856–5861 (2001).
59. V. F. Langness, *et al*. Cholesterol-lowering drugs reduce APP processing to Aβ by inducing APP dimerization. *Mol. Biol. Cell* **32**, 247–259 (2021).
60. E. Barbero-Camps, A. Fernández, L. Martínez, J. C. Fernández-Checa, A. Colell, APP/PS1 mice overexpressing SREBP-2 exhibit combined Aβ accumulation and tau pathology underlying Alzheimer's disease. *Hum. Mol. Genet.* **22**, 3460–3476 (2013).
61. P. J. Barrett, *et al*. The amyloid precursor protein has a flexible transmembrane domain and binds cholesterol. *Science* **336**, 1168–1171 (2012).
62. L. Puglielli, R. E. Tanzi, D. M. Kovacs, Alzheimer's disease: The cholesterol connection. *Nat. Neurosci.* **6**, 345–351 (2003).
63. O. Sano *et al*., ABCG1 and ABCG4 suppress γ-secretase activity and amyloid β production. *PLoS One* **11**, e0155400 (2016).
64. A. A. Escamilla-Ayala *et al*., Super-resolution microscopy reveals majorly mono- and dimeric presenilin1/γ-secretase at the cell surface. *eLife* **9**, e56679 (2020).
65. C. Wang *et al*., Selective removal of astrocytic APOE4 strongly protects against tau-mediated neurodegeneration and decreases synaptic phagocytosis by microglia. *Neuron* **109**, 1657–1674.e7 (2021).
66. E. M. Reiman *et al*.; Alzheimer's Disease Genetics Consortium, Exceptionally low likelihood of Alzheimer's dementia in APOE2 homozygotes from a 5,000-person neuropathological study. *Nat. Commun.* **11**, 667 (2020).
67. J. F. Arboleda-Velasquez *et al*., Resistance to autosomal dominant Alzheimer's disease in an APOE3 Christchurch homozygote: A case report. *Nat. Med.* **25**, 1680–1683 (2019).
68. S. Ye *et al*., Apolipoprotein (apo) E4 enhances amyloid β peptide production in cultured neuronal cells: apoE structure as a potential therapeutic target. *Proc. Natl. Acad. Sci. U.S.A.* **102**, 18700–18705 (2005).
69. Y. I. Miller, J. M. Navia-pelaez, M. Corr, T. L. Yaksh, Lipid rafts in glial cells: Role in neuroinflammation and pain processing. *J. Lipid Res.* **61**, 655–666 (2020).
70. Y.-W. A. Huang, B. Zhou, M. Wernig, T. C. Südhof, ApoE2, ApoE3, and ApoE4 differentially stimulate APP transcription and Aβ secretion. *Cell* **168**, 427–441.e21 (2017).
71. D. Milovanovic *et al*., Hydrophobic mismatch sorts SNARE proteins into distinct membrane domains. *Nat. Commun.* **6**, 5984 (2015).
72. M. J. Shipston, Ion channel regulation by protein palmitoylation. *J. Biol. Chem.* **286**, 8709–8716 (2011).
73. A. Nayebosadri, E. N. Petersen, C. Cabanos, S. B. Hansen, A membrane thickness sensor in TREK-1 channels transduces mechanical force. *SSRN* [Preprint] (2018). https://papers.ssrn.com/sol3/papers.cfm?abstract_id=3155650. Accessed 3 August 2021.
74. E. N. Petersen, M. A. Pavel, H. Wang, S. B. Hansen, Disruption of palmitate-mediated localization; a shared pathway of force and anesthetic activation of TREK-1 channels. *Biochim. Biophys. Acta Biomembr.* **1862**, 183091 (2020).
75. E. N. Petersen, *et al*. Phospholipase D transduces force to TREK-1 channels in a biological membrane. *bioRxiv* [Preprint] (2019). https://www.biorxiv.org/content/10.1101/758896v1. Accessed 3 August 2021.
76. A. B. Reiss *et al*., Cholesterol in neurologic disorders of the elderly: Stroke and Alzheimer's disease. *Neurobiol. Aging* **25**, 977–989 (2004).
77. S. Moon *et al*., Spectrally resolved, functional super-resolution microscopy reveals nanoscale compositional heterogeneity in live-cell membranes. *J. Am. Chem. Soc.* **139**, 10944–10947 (2017).
78. H. Wang *et al*., Regulation of beta-amyloid production in neurons by astrocyte-derived cholesterol. *Mendeley Data*, V1. https://doi.org/10.17632/4s373hyhj6.1. Deposited 26 July 2021.